IEEE Access
Multidisciplinary | Rapid Review | Open Access Journal

IEEE ENGINEERING IN MEDICINE AND BIOLOGY SOCIETY SECTION

Received January 26, 2021, accepted April 2, 2021, date of publication April 13, 2021, date of current version April 27, 2021.

Digital Object Identifier 10.1109/ACCESS.2021.3072977

A Phonography-Based Method Improved by Hidden Markov Model for Fetal Breathing Movement Detection

MÁRTON ÁRON GODA[1], (Member, IEEE), AND TAMÁS TELEK[2]
[1]Faculty of Information Technology and Bionics, Pázmány Péter Catholic University, 1083 Budapest, Hungary
[2]St. Margaret Hospital, 1032 Budapest, Hungary

Corresponding author: Márton Áron Goda (goda.marton.aron@itk.ppke.hu)

ABSTRACT This paper proposes a novel phonography-based method for Fetal Breathing Movement (FBM) detection by its excitation sounds. It requires significantly less effort than the current procedures, and it allows long-term measurement, even at home. More than 50 pregnancies in the third trimester were examined, for a minimum of 20 minutes, taking synchronous long-term measurements using a commercial phonocardiographic fetal monitor and a 3D ultrasound machine. To analyze the gained chaotic signal, the frequency band was split into single test-frequencies in the 15–35 Hz frequency band, and their signal-free (silent) zones were regarded as the starting point (SP) of the next motions. The analysis made other disturbing signals, such as fetal hiccups, trunk rotation and limb movements, or maternal heart beats, distinguishable. The dominant test-frequencies of the analysis were predicted by a Hidden Markov Model (HMM). The SPs of the motion units (episodes) were determined by some features of the FBM, applying weighting factors. The recorded material lasted for 16 hours altogether (with nearly 3.5 hours of FBM). Based on the results of HMM method, nearly 7500 FBM episodes were identified in the phonogram signal with an average length of 0.96±0.13 seconds. The procedure for phonography-based breathing movement detection can be combined with a fetal heart activity measurement, and thus allows very intensive, long-term monitoring of the fetus.

INDEX TERMS Fetal breathing movement (FBM), phonography, sonography, Biophysical Profile (BPP), HMM, dominant test-frequency.

I. INTRODUCTION

The widespread popularity of ultrasound imaging resulted in more detailed measurements of fetal activity with a higher resolution and identified the variability of Fetal Breathing Movement (FBM) [1]. However, early scientific results did not clarify all aspects of FBM, even though it became a meaningful indicator for fetal well-being. This was demonstrated by the Biophysical Profile (BPP), which uses FBM as an important index during pregnancy [2]. The main problem with all of these measurements was that they took a long time and required medical expertise.

New possibilities have since arisen with the improvement of sonography and phonocardiography [3], dealing with special aspects of FBM detection such as the cross-correlation between breathing and Fetal Heart Rate (FHR) variations, or the analysis of inspiratory and expiratory data [4]. Research also extended to fetal hiccups [5], [6]. Meanwhile, the issues of Sudden Infant Death Syndrome (SIDS) [7] and Intrauterine Growth Retardation (IUGR) inspired further studies investigating fetal activity [8], [9]. FBMs also play an important role in the development of the respiratory center in the brainstem [10]. The latest solution seems to be the application of accelerometers [11], used mainly for measuring the fetal diaphragm's position. Thus, after cancelling out other noises – such as sounds of respiration and heart beats – one can arrive at a rough estimation for fetal breathing. The FBM episodes still cannot be distinctly identified this way. Nevertheless, a new technical possibility, the phonographic method [12] has revolutionized the field of fetal measurements.

This study presents a testing method which involves fetal examinations, which might last for as long as 24 hours, conducted via a mobile network, being in no way constrained

The associate editor coordinating the review of this manuscript and approving it for publication was Alessandra Bertoldo.

by the limitations normally associated with hospital examinations. It is applicable especially when a large number of tests and long-time measurements are needed, typically involving home monitoring for the instant identification of FBMs using appropriate features in the 15–35 Hz frequency band [13].

The Hidden Markov Model is used for unobservable states of Markov processes. The HMM was applied for adult heart sound analysis by Springer *et al.* [14], Lima and Barbosa [15], and Schmidt *et al.* [16]. The Markov-Switching Model was also used by Noman *et al.* [17] for adult heart sound segmentation and classification. These results inspired us to implement the HMM in this work for the dominant test-frequency prediction. If one considers the required large computation capacity for the search of real SPs, one may well assume that this task may be simplified by using the HMM. In this way, based on previously observed and valid silent-zones, the timing of the next one may be predicted, thereby decreasing the number of test-frequencies that need to be examined.

A. INVESTIGATIONS OF FETAL BREATHING MOVEMENT

The sound of FBM is the produced by the movement of the diaphragm by mobilizing additional tissue and the surrounding amniotic fluid. It is not related to the fetal oxygen uptake; its name arises from the fact that it is a precursor to a training for postpartum breathing. It starts in an early stage of pregnancy, but it develops permanently towards the end of the third trimester and shows differences according to sex.

The movement of the diaphragm is an approximately 1-second-long back-and-forth motion in a signal around 2-3 Hz, and its corresponding filtering is extremely difficult due to the very narrow bandwidth. Therefore, sonography has been chosen for this motion detection. However, the basic method is extremely costly, as professionals are required to carry out the measurements for a long time, because the motion occurs randomly.

The phonographic method [13], [18] offers a new possibility for FBM detection that can measure the secondary excited sounds, and identify these movements (hereinafter *episodes*) according to their distribution. So, we must emphasize that this is a secondary perception of FBMs. Consequently, the measured signal moves its surrounding area in different ways; it is chaotic and so cannot be handled by traditional signal processing methods. Only a complex method can solve this problem.

Three FBMs are shown in Figure 1 in a phonographic signal, where a low signal intensity is followed by an ascending intensity of the contraction and a descending intensity of the relaxation phase. The relaxation involves much less effort on the part of the fetus; therefore, it is much more uncertain than the contraction.

Identifying the location of the starting of movement in the signal is the most reliable way to segment this chaotic signal. Thus, we assume that the system is at rest before the intensity rises. There is no movement, and signal intensity is also minimal. The signal level of this zone (hereinafter referred to as the *silent-zone*) is therefore assumed to be zero.

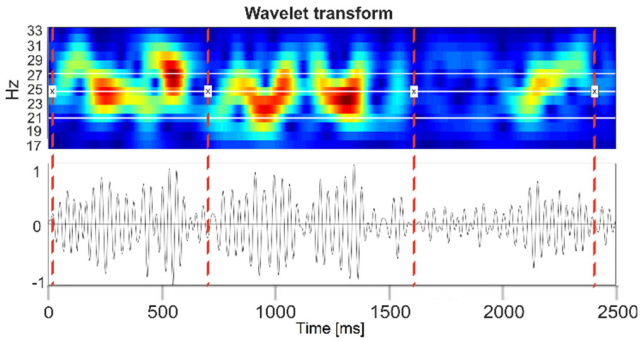

FIGURE 1. Three FBM episodes in the phonogram signal between 15–35 Hz. The episodes are separated by decrease intensity, which are also marked by red dashed lines. While the first two episodes are clearly visible, the 3rd is only partially so.

Accordingly, not all excited signals attenuate because of the previous motions at this time, and thus a signal (at a reduced level) will be measurable in this zone. This is shown in Figure 1, where three chaotic movements can be seen. At the first two movements, there is a well-established quiet-zone in the example. But the third episode is already a truncated episode, where instead of a normal form, a ''gasp for air''-like movement is produced.

Frequency-splitting (see 2.2 Frequency Splitting) was used for the evaluation of chaotic signals. This method has also been used for other chaotic biomedical signals, e.g. breathing, coughing, heart sound segmentation in adults [19]. In the present case, the attenuated frequency components are separated from the other remaining disturbed components. These attenuated signals indicate the starting points of FBMs with a relatively high certainty. Based on this, the objective is to discover these FBM episodes and determine their temporal distribution. This can give more nuanced information about fetal well-being.

B. THE SIGNAL TO BE MEASURED

The FBM is the rhythmic contraction and relaxation of the diaphragm. One unit of this is the *episode*, and the series of concatenated episodes forms the *epoch*. The epochs can be divided into smaller *episode groups*, separated by shorter breaks.

The episode itself is a chaotic signal (see Fig. 1), the epoch, on the other hand is quasi-periodic with 0.8–1.2 seconds of repetition time. The time-interval which separates the episodes is sometimes very short. Therefore, to determine all standalone episodes is very difficult. In fact, the main problem here is that this separating zone (called in the following the *silent-zone*) is not really a completely quiet zone, because some components of the excited sound components are not attenuated for even this very short time.

In general, the problem with the analysis of an episode is that it is hard to define exactly where it starts and where it finishes. This is due to the very short time-intervals between the two neighboring episodes, during which, theoretically, there is no movement; and consequently, there is no sound.

However, some components of the motion do not involve calm periods. Therefore, the episode may not be regarded as a perfect quiet-zone, but can only be treated as a silent-zone. The end of this zone incorporates the starting point (SP) of the episode, and its beginning is the former episode's end. This is illustrated in Figure 1 on a wavelet-transformed [20] time-frequency map, showing the remaining signals at the separating silent-zones, which refer to the *potential SPs*. The figure shows that the spectrum of the signal is delimited to the 15–35 Hz base-band, inside of which the whole analysis will be carried out. The detailed examination of the frequency bands of the phonographic signal is essential to FBM detection, which will be described in the following sections.

II. MATERIALS AND METHODS

A. MEASUREMENTS

The measuring setup is shown in Figure 2. The measurement is carried out using the analogous part of the commercially available Fetaphon2000 type phonocardiograph monitor (see Table 1) placed on the maternal abdomen with a belt. Its optimal position can be found by the audible sound of the fetal heart sounds.

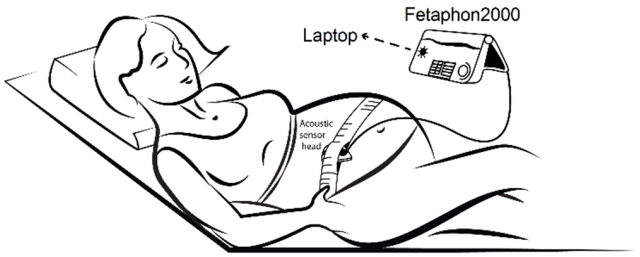

FIGURE 2. The measuring setup. The sound received by the Fetaphon-type acoustic sensor is preconditioned and transmitted to the laptop. For validation, a conventional 3D sonograph has been applied.

For the sake of validation, a Samsung UGEO-H60 type 3D Sonograph (with 400 ms sampling time and $1366 \times 768 \times 24$ bit resolution) was applied for the continuous observation of the diaphragm's contraction and relaxation, allowing thus the synchronous measurements of the received sounds.

TABLE 1. Fetaphon2000 fetal home monitor.

Sampling Time	Data Resolution	Bandwidth
3 ms	8 bit	15–100 Hz

The detected sound signal was amplified, filtered and digitized by the conventional preconditional circuit of the heart monitor of Table 1 with a $T_s = 3$ ms sampling time.

The recorded digital data were transmitted to a laptop or to a network (Internet or mobile network) for post-processing and evaluation (see Fig. 3).

The amplitude of the detected signals depends on the position of the fetus; therefore, with long-term examinations, the position of the sensor needs to be adjusted (appropriately by the mother) in time, whereby the gain in amplification within a given range can be corrected.

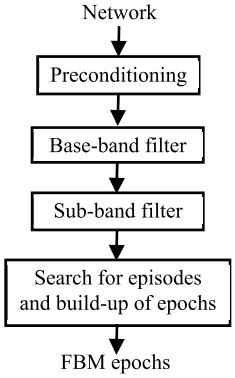

FIGURE 3. The modules of the FBM detection in the phonogram signal.

B. FREQUENCY SPLITTING

The most promising approach for FBM detection is the investigation of a chaotic signal at different frequency bands. The *test-frequencies* are between 15–35 Hz. This selected frequency band is scanned and evaluated by test-frequencies [17]. Least-squares type 20^{th} order linear phase band-pass FIR filters were applied with 4 Hz bandwidth.

Then from each of these, a test-frequency was selected marked f_m. In this way, the chaotic signal was substituted by single frequencies that are easy to handle. This method has successfully been applied in some other studies as well, for analyzing seemingly chaotic biomedical signals [22]. The principal exploration of the silent-zones is achieved by systematic scanning, which involves all the test-frequencies.

Some silent-zones should be related to the starts of the next episodes (see Fig. 1). The task is only to clarify which frequencies should be applied along the time function, and which silent-zone found should be selected as a potential SP from these chaotic signals. During those short time-intervals, the signal intensity is extremely low on most of the frequencies. There is no motion, and so a SP can be supposed, since a simultaneous disappearance of all frequency components is not otherwise probable.

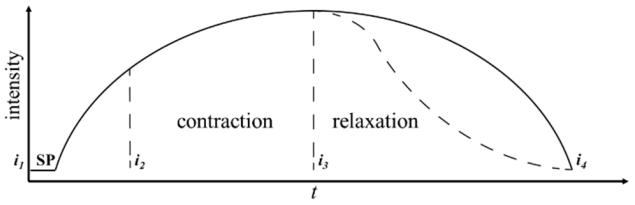

FIGURE 4. Illustration of the form of the mean intensity of FBM episodes.

C. FEATURE EXTRACTION OF THE STARTING POINTS

During feature extraction, the following process had to be carried out for all frequency components, splitting them so as to identify the starting points (SPs). In the process of detailed and rigorous investigation of the chaotic-type records, the selected promising features were to a discernible extent the intensities of a given part of the record measured on a given test-frequency. They are now marked as $F(m,i)$ where

m marks the test-frequencies and i stands for the location of features in the phonogram signal.

Figure 4 schematically shows the average intensity of FBM episodes. In the case of i_4, the dashed line indicates that the relaxation sound is much more uncertain than the contraction sound; therefore, its average intensity fluctuates.

The first of these features is the remaining signal level on the silent-zone, which may be marked as a potential starting point [13]. To extract these features, scanning all $s_m[i]$ test-frequencies, Equation (1) provides the F_1 feature for the m^{th} test-frequency.

$$F_1\,(m, z, i_1) = w_1(m, z)/\sum_{i=i_{SP}}^{i_1} \frac{abs\,(s_m\,[i])}{i_{SP} - i_1} \tag{1}$$

where z is the actual index of investigated episode at the m^{th} test- frequency, $s_m[i]$ is the sampled sound signal at the m^{th} test-frequency, i_{SP} is the end-point of the $(i_{SP} - i_1) =$ 30 ms long silent-zone and $w_1(m, z)$ is the weighted factor signal at the m^{th} test-frequency. The feature is inverse in character, since the high certainty of this feature requires a low remaining signal level. Before the usage of analog-digital conversion, the phonogram signal level is intelligently set by an amplifier due to any event detection.

The features F_{2-4} represent the signal level (intensities) within given time periods during different stages of the episodes, expressed by the general Equation (2).

$$F_k\,(m, z, i_k) = w_k(m, z)\sum_{i=i_{SP}}^{i_k} \frac{abs\,(s_m\,[i])}{i_k - i_{SP}} \tag{2}$$

where $w_k(m, z)$ is the weighted factor and z is the actual index of investigated episode at the m^{th} test-frequency. Here $F_2\,(k = 2)$ represents the $(i_2 - i_{SP}) = 0.1$ s length rising period just after the SP with the end point of i_2. Similarly, the $\left(i_3 - i_{sp}\right) = 0.5$ s long $F_3\,(k{=}\,3)$ yields the intensity of first half of the episode. According to F_4, the whole intensity (power) of the total length of the actual episode is applied by the average $(i_4 - i_{SP}) = 1$ s time value.

The features essentially express the power distribution produced by the given weighted factor. The actual value of the weight factors can be determined according to the already accepted episodes (see Equation 3).

$$w_k(m, z) = \sum_{z-n}^{z-1} \frac{1}{F'_k\,(m, z, n_k)} \tag{3}$$

where $w_k(m, z)$ denotes the weighted factor of the current feature, $F'_k\,(m, z, n_k)$ refers to the feature of the already accepted episodes, n is a running variable, k marks the feature indexes, N is the number of the examined episodes, $n < N$, and z-N is the index of the initial episode.

TABLE 2. The default weighted factors.

w_1	w_2	w_3	w_4
$100/I_h$	$2/I_h$	$1/(I_h \times 2)$	$1/(I_h \times 3)$

In Table 2, the initial value of the weighted factors is determined by provisorily applied synchronous measure I_h, which indicates average fetal heart sound intensity. The weighted factors are continuously updated according to Equation (3).

D. SUMMARIZED EVALUATION OF THE MEASURED FEATURE

The global value of the examined SPs is denoted by Equation (4), where $G_F(m,z,i_n)$ is the sum of the presented F_{1-4} features.

$$G_F\,(m, z, i_{\mathrm{n}}) = \sum_{n=1}^{4} F_n\,(m, z, i_{\mathrm{n}}) \tag{4}$$

where n is the number of (F_{1-4}) features, m signifies the test-frequencies, z is the actual index of investigated episode at the m^{th} test-frequency. The total output of this process will determine a) the acceptance of a silent-zone as a real SP, or b) their retention as a other potential SP, or c) its rejection. The upper and lower limits are $G_{F,max}$ and $G_{F,min}$. If the G_F is accepted, but intensity is moderate, then it can be used for interpolation of hypothetical SPs (see 2.6).

$$\mathrm{SP} = \begin{cases} \text{accept, if} & G_F > G_{F,max} \\ \text{retain, if} & G_{F,min} < G_F < G_{F,max} \\ \text{reject, if} & G_F < G_{F,min} \end{cases} \tag{5}$$

The limits of the features, the corresponding weight as well as the global levels are initial (default) values. They may be adjusted after every 8-10 episodes taking into account the measured features and the distribution of the SPs [13].

E. THE PREDICTION OF DOMINANT TEST-FREQUENCIES BY HMM

The evaluated form of FBM intensity is represented by the factor G_F at the different test-frequencies. Based on this, the potential SPs can be determined that mark the start of episodes. However, the spectrum of the SPs is also continuously changing; thus the additional *sub-bands* (also called *test-frequencies*) are used in the previously filtered 15–35 Hz phonographic signal. In many cases, a so-called *dominant test-frequency* will be observed, on which the SPs can be also well detected. The accurate observation of the potential SPs results in the transitions states of a Markov process, which predict the current dominant test-frequency bands at every time t.

The $\boldsymbol{S}^F$ state space marks the dominant test-frequency states, which are not directly observable, thus the series of dominant test-frequencies can be considered as a hidden Markov process (HMM).

$$S^F = \{\varphi_1, \varphi_2, \ldots, \varphi_{nf}\} \tag{6}$$

where nf is the number of frequency bands, and $\varphi, \varphi_2, \ldots, \varphi_{nf}$ are the applied test-frequencies (in our case 21 Hz, 23 Hz, 25 Hz, 27 Hz, 29 Hz). Although, the dominant test-frequency is unknown at a given moment, the probability of it can be also inferred from the previously determined $\boldsymbol{S}^D$ states.

The inputs of the Markov process are given from the location of potential SPs at each test-frequency. The outputs of the

model are the next dominant test-frequency and its duration. The time-intervals *(duration)* between SPs determine the $\mathbf{S}^D$ state space that results in a series of time-intervals states at each test-frequency. The distribution of the time-intervals between the potential SPs was classified into four different states.

$$\mathbf{S}^D = \{\delta_1, \delta_2, \delta_3, \delta_4\} \tag{7}$$

where $0 \leq \delta_1 < 0.3$ s, $0.3 \leq \delta_2 < 0.75$ s, $0.75 \leq \delta_3 < 1.2$ s and $\delta_4 \geq 1.2$ s. These states were determined according to earlier empirical experiences, where δ_2 and δ_3 refer to the diaphragm contraction (0.3–0.75 sec) and relaxation (0.75–1.2 s) in the FBM episodes. The boundary time-interval states are δ_1 and δ_4 (0–0.3 and over 1.2 s) that are used for the other silent-zones.

Based on these, the model can be defined as follows. Let $F^t(\tau)$ be a Markov chain at time t with state-space S^F, which refers to the previously defined test-frequency states. The time-variable of the Markov chain is $\tau \in \{1, \ldots, \tau_{max}\}$, where τ_{max} is the maximum window size of the examined time interval.

The Markov model are the transition probabilities $A_{ij}(t)$, which determines the transition probability of the φ_i frequency state from the φ_j frequency state at the current time instance. Let us denote the transition matrix of the Markov chain F^t by A_{ij}, that is the (i, j) elements of $A_{ij}(t)$ are

$$A_{ij}(t) := P(F^t(\tau) = \varphi_i | F^t(\tau - 1) = \varphi_j) \quad i, j \in 1, .., nf \tag{8}$$

where nf is the number of frequency bands, $F^t(\tau)$ is the test-frequencies vector defining states at time t within the τ time window. The A_{ij} derives from transition of potential SPs at the different test-frequencies, namely the interesting changing part of fetal activity can be characterized by the potential SPs.

Let $D^t(\tau)$ be a HMM for a given time-window $t \in N$ with state-space $\mathbf{S}^D$, which refers to the previously defined time-interval states. The time variable of this process $\tau \in \{1, \ldots, \tau_{max}\}$, where τ_{max} is the maximum time window-size.

The relative postion of the potential SPs were investigated at the different test-frequencies. The $B_{ij}(t)$ determines the δ_i interval probabilities from the φ_j frequency states at the current time instance. Let us denote the transition matrix of the HMM D^t by B_{ij}, that is the (i, j) elements of $B_{ij}(t)$ are

$$B_{ij}(t) := P(D^t(\tau) = \delta_i | F^t(\tau) = \varphi_j), \quad i \in 1, .., 4, \ j \in 1, .., nf \tag{9}$$

where nf is the number of frequency bands, $D^t(\tau)$ is the time-interval state vector defining states at time t for the τ time window. B_{ij} describes the probabilities of interval-states between the silent-zones at the different test-frequencies.

The A_{ij} and B_{ij} transition matrices can be used to determine a C_{ij} transition matrix that designates the location of the dominant test-frequency and its length (see Equation (10)). The transition matrices were inspected for each $\tau \in \{1, \ldots, \tau_{max}\}$ time. According to the Bayes theorem, the conditional probability of the dominant sub-bands is given by the occurrence of the interval states.

$$\begin{aligned} C_{ij}(\mathrm{t}) &:= P(F^t(\tau) = \varphi_i | D^t(\tau) = \delta_j) = \\ &= P\left(D^t(\tau) = \delta_j \,|\, F^t(\tau) = \varphi_i\right) \frac{P\left(F^t(\tau) = \varphi_i\right)}{\mathrm{P}\left(D^t(\tau) = \delta_i\right)} \end{aligned} \tag{10}$$

where $i \in 1, .., nf$, $j \in 1, .., 4$, and nf is the number of frequency bands, furthermore

$$P\left(D^t(\tau) = \delta_j \,|\, F^t(\tau) = \varphi_i\right) = B_{ij}(t) \tag{11}$$

where the $\mathrm{P}\left(D^t(\tau) = \delta_i\right)$ probability has been estimated by

$$P\left(\widehat{D^t(\tau)} = \delta_i\right) = \frac{\sum_{j=1}^{4} B_{ij}(t)}{\sum_{i=1}^{n} \sum_{j=1}^{4} B_{ij}(t)} \tag{12}$$

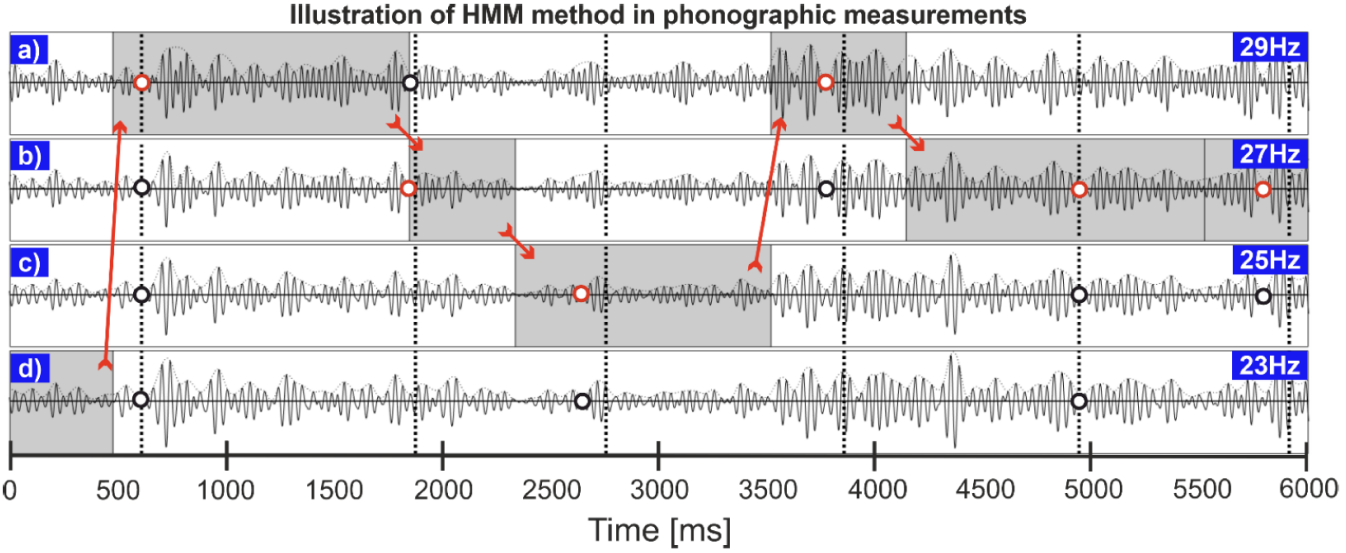

FIGURE 5. The output of the HMM is the predicted dominant test-frequency and its time-window. Four frequency state-transitions are depicted in subfigures a)–d). The highlighted background refers to the actual dominant test-frequency. According to the G_F global values, the red circles mark the SPs of HMM test-frequencies.

and finally $C_{ij}(t)$ probability matrix is estimated by

$$C_{ij}(t) \approx \hat{C}_{ij}(t) = \hat{B}_{ij}(t) \frac{P\left(F^t(\tau) \mid \varphi_i\right)}{P\left(\widehat{D^t(\tau) = \delta_i}\right)} \times i \in 1, \ldots, nf,\ j \in 1, \ldots, 4 \quad (13)$$

where nf is the number of frequency bands.

The $C_{ij}(t)$ probability matrix is defined by frequency and time-interval transition matrices, and this can predict the next dominant sub-band at every t time (see Fig. 5). Here the SPs as the start of the next FBM episode are the most appropriately detectable. The state-transition matrix data are continuously updated during the evaluation. Although the defined state transition matrices of the HMM have been implemented in Matlab for the graphic visualization and the evaluation; they are also capable of real-time data processing.

The applied model made episode detection more efficient using the dominant test-frequencies and the temporary exclusion of the other test-frequencies. In this way, the number and size of test-frequencies can be optimized, which results in efficient data processing.

F. INTERPOLATION OF SPs

As shown above, the most reliable tool for identifying an episode is locating their SP. This requires the confirmation of the selected SP. The situation is more critical if there is no SP. In this case, the sampled point will be borrowed as a hypothetical SP, whose distance from the neighboring SPs is nearly identical.

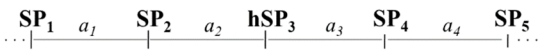

FIGURE 6. Illustration of the interpolation applied on the hypothetical starting point (hSP_3).

During the interpolation, neighboring SPs are used for the hypothetical SP (hSP) as shown in Figure 6. In this case, the following expression

$$hSP_3 = SP_2 + 1/3\,(a_1 + a_4 + (a_2 + a_3)/2) \quad (14)$$

can be used, knowing that it does not impact the number of episodes. Most movements are tiring and exhausting for the fetuses. The occurrence of a hSP may be an explanation for this, and it refers to the short break between the movements.

G. FLOW CHART AND ITS BLOCKS

The flow diagram and building blocks of the FBM detection are shown in Figure 7, where the feedback marks the repetitions for all test-frequencies. The short descriptions of the numbered blocks are as follows.

1) Prepare the setup and place the phonographic sensor onto the maternal abdomen wall to the optimal position, appropriately near the fetus. Before the identification of a FBM, the detection of fetal heart sound is essential. In addition, adjustment of the amplification of the recording device to the estimated level of the FBM is required. Finally, the actual level of noise and other disturbing sounds should be established; if these are regarded to be too high, the whole measurement should be postponed.
2) Begin the pre-filtering of the received signal to the used base frequency band (15–35 Hz) and then produce the narrow test-frequencies (BW = 4 Hz), which cover the whole frequency band.
3) Comprehensive scanning of all the selected frequencies is carried out to detect all potential SPs according to the features F_{1-4}; and the level of the following rising parts according to Equations 1–2. Scanning the potential SPs in all test-frequencies is done using the G_F global value.
4) Based on the transition matrices, the HMM estimates the most dominant test-frequency band to find the potential SPs.
5) Interpolations of SPs are applied for the insertion of hypothetical SPs.

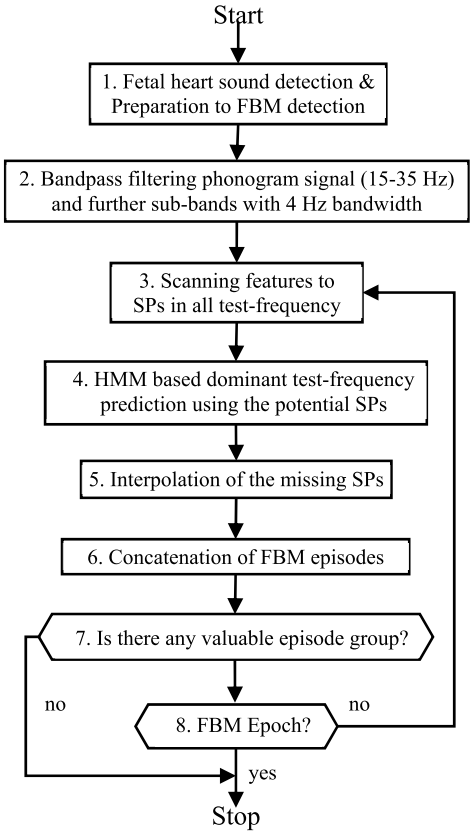

FIGURE 7. The phonographic signals are evaluated for the FBM search in the following steps. After the basic time and frequency analysis, the features are used for episode detection. The HMM predicts the dominant test-frequencies. Interpolation helps to find the missing SPs, which results in contiguous episode groups. This process is finished if there is no valuable episode group, or if the criteria of an FBM epoch are fulfilled for the given time window.

6) The accepted hypothetical SPs are concatenated so that they can form the FBM episode groups.
7) If there is any valuable episode group for FBM epochs, then the process will be continued; otherwise, the process is ended.
8) If the FBM episode group fulfills the criteria of epochs, then the processing is also finished. Otherwise, the FBM features are scanned with new weighted factors.

H. VALIDATION

The success of fetal monitoring is based on many years of experience. Originally, the FBM was a disturbing signal in the phonogram, which became a by-product of earlier research. Although hundreds of suspected FBMs have been recorded over time, we had to make synchronous measurements to specify and validate them as well (see Table 3). St. Margaret Hospital, Budapest, supported our research with medical consultations of more than 50 synchronous measurements using sonographic and phonographic recording. The recorded material lasted for 16 hours altogether (with nearly 3.5 hours of FBM).

TABLE 3. Summary of examined fetuses.

Sex	No.	Fetal age	Fetal weight	Gross FM	FBM
female	25	34±3 week	2250±570 g	56 min	113 min
male	25	34±3 week	2400±670 g	77 min	91 min

This table summarizes 50 synchronous measurements made by phonographic equipment and a 3D ultrasound machine. The main influencing factors of FBM are the age and the weight of fetus as well as their other movements.

Each measurement lasted for an average of 20 minutes. The phonographic device was placed near the fetal heart sound on the mother's abdomen. During the scanning, the moving point on the diaphragm was continuously followed with sonography.

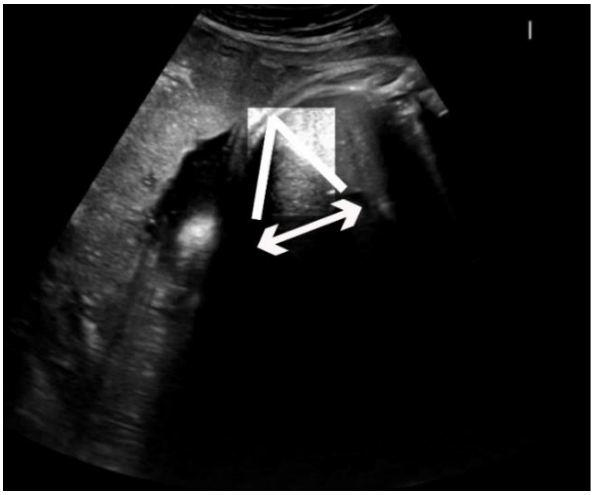

FIGURE 8. The sonographic measurement via 3D ultrasound. During contraction, the image is darker around the diaphragm, and it is brighter when relaxation occurs.

The image of one contraction and the following relaxation is shown in Figure 8. It was identified in the gray shaded ultrasound video. In the case of FBM contraction, the image is darker around the diaphragm, and it is brighter during the relaxation. Based on this, the FBMs were reconstructed. Each movement was labelled manually on the second recording channel parallel to the phonographic signal as well. The examinations were performed by proficient sonographers, and the recorded signals were also double checked after the measurements. The exact time of this electronically designated motion was also captured by the photogrammetric method on the video. It is clear that the sonographically marked episodes and ones selected by acoustic signal processing were almost the same.

III. RESULTS

Based on results of the HMM method, nearly 7500 FBMs were identified on in the recorded phonogram signal (see Table 4). The recorded material lasted for 16 hours altogether (with nearly 3.5 hours of FBM). However, the measurements revealed that the epochs can be even up to 1–2 minutes long, but the length and intensity of their episodes are dynamically changing. This effect also correlates strongly with fetal well-being.

The BPP prescribes a 30-second-long FBM during the 30 minute examination. However, our measurements proved that the FBM epochs are formed by smaller episode groups. The episode groups have to consist of at least 2–3 members, which become longer and more intense towards the end of pregnancy.

Regarding to BPP test, more than 95% of the episode groups are detectable in the phonogram signal. However, from the medical point of view, the significance of completely separate short episode groups is still unknown. The identification of these episode groups is also a challenge both in sonographic and phonographic signals.

TABLE 4. Evaluation of the detected episodes.

No. episode groups (pc)	1221
No. episodes (pc)	7536
Mean of episode length (sec)	0.96±0.13

Due to interpolation, many shorter FBM episode groups are also assessable in the case of phonogram methods. This step was essential for future evaluation, because the FBM epochs are not a series of homogenous episodes. They are rather formed from different mini-epoch groups. This fact was also proved by our sonographic measurements.

The average intensity of FBM episodes is at least 3–4 times higher than that of heart sounds. The measurements proved that due to the relatively high intensity of the FBM, it is not disturbed by maternal heart sound or fetal heart sound. Of course, other strong movements of the fetus (eg. trunk rotation, fetal kicks, flutters, swishes) make the measurement completely impossible – in this case it must be postponed. The measurements largely depend on the position of the sensor head; therefore, it is good if the phonogram is located as close as possible to the fetus. The reliable detection of

fetal heart sounds is essential for the determination of FBM. Namely, the intensity of these signals could be considered as a reference.

TABLE 5. Dominant test-frequencies distribution.

Females	21 Hz	23 Hz	25 Hz	27 Hz	29 Hz
29–31 w	7.0%	12.7%	11.8%	23.1%	45.4%
32–36 w	10.4%	8.2%	12.8%	20.6%	48.0%
37–39 w	12.9%	10.6%	12.7%	21.2%	42.7%
Males					
29–31 w	7.6%	8.0%	11.4%	19.0%	54.0%
32–36 w	7.7%	7.7%	11.3%	22.6%	50.7%
37–39 w	5.6%	8.4%	12.7%	22.7%	50.6%

In Table 5, distribution is shown of the HMM predicted dominant frequencies by sex and weeks. It is clearly visible that the 29 Hz test-frequency is the most dominant one; however, the other frequency bands should not be completely ignored. This is very important in order to justify that the FBMs are not totally chaotic, which legitimates the usage of HMM.

IV. DISCUSSION

A Phonography-Based method have been improved by HMM for FBM detection. The implemented method is based on the extracted features of the FBMs in the 15–35 Hz frequency band. The transition matrices of silent-zones and the different frequency-states is suitable to select the dominant test-frequencies, where the real SPs as the start of the next FBM episode are detectable.

The phonographic measurement takes place by means of a noninvasive acoustic sensor on the maternal abdomen wall, placed appropriately near the fetus. Hence, the system may be used even at home to measure the FHR value fully with all indices and variability, including some Congenital Heart Disease (CHD) markers and the FBM. This provides a monitoring method for the pregnancy in the third trimester in a convenient way [23]. Overall, the following observations can be made:

a) The extracted features and HMM can determine the FBMs in the signals regarding to BPP test.
b) The homogeneous long-term FBM epochs are very rare and the episodes are constantly changing.
c) In some longer episodes, at the end the intensity of the epochs decreases, which implies that the given fetus has become exhausted.
d) With some fetuses very short, ''gasp for air''-like movements were found to be frequent; this may be symptomatic of the irregularity of the movements.
e) Position changes on the part of the fetus result in false measurements; hence, the mother should manually adjust the acoustic sensor head, especially at long-term home measurements.
f) The fetal physical efforts have been investigated in the different gestational ages and the dominant test-frequency distribution of FBMs are nearly same in case of female and male fetuses.
g) The experiments demonstrated that due to the common test head with a heart monitor, the FBM measurements might be combined with further fetal examinations.
h) Newborn babies are strongly affected by the intrauterine growth retardation (IUGR), and the major risks are preterm birth and respiratory insufficiency. Finally, the understanding of the link between FBM and sudden infant death syndrome (SIDS) can be open new perspectives in field of fetal monitoring.

V. CONCLUSION

The results of the HMM method have shown that fetal phonography is a suitable tool to discover the FBM epochs. This research has broadened our horizons in this field. The episode groups of FBMs provide an explanation for the continuously changing fetal activities. However, long-term conclusions can only be drawn from further research.

The phonogram is already an available tool for fetal telemedicine (see Fetaphon2000). Nevertheless, much larger databases of phonograms would be needed for further tool developments and the reliable assessment of fetal well-being. Previously, the phonographic measurement indicated the abnormal fetal activities during home monitoring, but the verification of sonographic measurement was too late to rescue the life of the fetus. Unfortunately, the snapshot measurements cannot provide a comprehensive view about the real condition of the fetus.

Since phonography allows long-term measurement at home, it offers a more accurate picture about fetal well-being. It could prevent intrauterine death in the last trimester, which carries plenty of risk factors. This research area is still immature. Nevertheless, telemedicine is expected to play an increasing role in the near future.

ABBREVIATIONS

BPP	Biophysical profile
FBM	Fetal breathing movement
FHR	Fetal heart rate
FIR	Finite Impulse Response filter
SP	Starting point of FBM episode

Funding: This research was funded by Pázmány Péter Catholic University.

Institutional Review Board Statement: The study was conducted according to the guidelines of the Declaration of Helsinki, and approved by Ethics Committee of St. Margaret Hospital, Budapest.

Informed Consent Statement: Informed consent was obtained from all subjects involved in the study.

Conflicts of Interest: The authors declare no conflict of interest.

ACKNOWLEDGMENT

The authors would like to thank the technical support of Pázmány Péter Catholic University and the medical support of St. Margaret Hospital, Budapest, for helping with the sonographic measurements.

REFERENCES

[1] J. Andrews, J. Shime, D. Gare, J. Salgado, and G. Whillans, "The variability of fetal breathing movements in normal human fetuses at term," *Amer. J. Obstetrics Gynecol.*, vol. 151, no. 2, pp. 280–282, Jan. 1985.
[2] J. G. Lalor, B. Fawole, Z. Alfirevic, and D. Devane, "Biophysical profile for fetal assessment in high risk pregnancies," *Cochrane Database Systematic Rev.*, no. 1, Jan. 2008, Art. no. CD000038, doi: 10.1002/14651858.CD000038.pub2.
[3] P. Chetlur Adithya, R. Sankar, W. A. Moreno, and S. Hart, "Trends in fetal monitoring through phonocardiography: Challenges and future directions," *Biomed. Signal Process. Control*, vol. 33, pp. 289–305, Mar. 2017, doi: 10.1016/j.bspc.2016.11.007.
[4] J. Florido, M. C. Padilla, V. Soto, A. Camacho, G. Moscoso, and L. Navarrete, "Photogrammetry of fetal breathing movements during the third trimester of pregnancy: Observations in normal and abnormal pregnancies," *Ultrasound Obstetrics Gynecol.*, vol. 32, no. 4, pp. 515–519, Sep. 2008, doi: 10.1002/uog.5329.
[5] J. C. Dornan, J. W. K. Ritchie, and S. Ruff, "The rate and regularity of breathing movements in the normal and growth-retarded fetus," *BJOG, Int. J. Obstetrics Gynaecol.*, vol. 91, no. 1, pp. 31–36, Jan. 1984.
[6] B. H. Kumar, "A fuzzy expert system design for analysis of body sounds and design of an unique electronic stethoscope," *Biosens. Bioelectron.*, vol. 22, no. 6, pp. 1121–1125, Jan. 2007.
[7] P. Zemb, H. Gonçalves, J. Bellec, and J. Bernardes, "Prenatal observation of heart rate sequences presenting entropic analogies with sudden infant death syndrome: Preliminary report," *Proc. 26th IEEE Int. Symp. Comput.-Based Med. Syst.*, Dec. 2013, pp. 421–424.
[8] M. G. Signorini, A. Fanelli, and G. Magenes, "Monitoring fetal heart rate during pregnancy: Contributions from advanced signal processing and wearable technology," *Comput. Math. Methods Med.*, vol. 2014, pp. 1–10, Dec. 2014, doi: 10.1155/2014/707581.
[9] D. Sharma, S. Shastri, and P. Sharma, "Intrauterine growth restriction: Antenatal and postnatal aspects," *Clin. Med. Insights Pediatr.*, vol. 10, pp. 67–83, Dec. 2016, doi: 10.4137/CMPed.S40070.
[10] M. R. Inanlou, M. Baguma-Nibasheka, and B. Kablar, "The role of fetal breathing-like movements in lung organogenesis," *Histol. Histopathol.*, vol. 20, no. 4, pp. 1261–1266, 2005, doi: 10.14670/HH-20.1261.
[11] E. Ryo and H. Kamata, "Fetal movement counting at home with a fetal movement acceleration measurement recorder: A preliminary report," *J. Maternal-Fetal Neonatal Med.*, vol. 25, no. 12, pp. 2629–2632, Dec. 2012, doi: 10.3109/14767058.2012.704449.
[12] F. Kovács, C. Horváth, Á. T. Balogh, and G. Hosszá, "Fetal phonocardiography—Past and future possibilities," *Comput. Methods Programs Biomed.*, vol. 104, no. 1, pp. 19–25, Oct. 2011, doi: 10.1016/j.cmpb.2010.10.006.
[13] F. Kovacs, M. A. Goda, G. Hosszu, and T. Telek, "A proposed phonography-based measurement of fetal breathing movement using segmented structures with frequency splitting," in *Proc. 42nd Annu. Int. Conf. IEEE Eng. Med. Biol. Soc. (EMBC)*, Montreal, QC, Canada, Jul. 2020, pp. 4483–4486.
[14] D. B. Springer, L. Tarassenko, and G. D. Clifford, "Logistic regression-HSMM-based heart sound segmentation," *IEEE Trans. Biomed. Eng.*, vol. 63, no. 4, pp. 822–832, Apr. 2016, doi: 10.1109/TBME.2015.2475278.
[15] C. S. Lima and D. Barbosa, "Automatic segmentation of the second cardiac sound by using wavelets and hidden Markov models," in *Proc. 30th Annu. Int. Conf. IEEE Eng. Med. Biol. Soc.*, Vancouver, BC, Canada, Aug. 2008, pp. 334–337.
[16] S. E. Schmidt, C. Holst-Hansen, C. Graff, E. Toft, and J. J. Struijk, "Segmentation of heart sound recordings by a duration-dependent hidden Markov model," *Physiol. Meas.*, vol. 31, no. 4, pp. 513–529, Apr. 2010, doi: 10.1088/0967-3334/31/4/004.
[17] F. Noman, S.-H. Salleh, C.-M. Ting, S. B. Samdin, H. Ombao, and H. Hussain, "A Markov-switching model approach to heart sound segmentation and classification," *IEEE J. Biomed. Health Informat.*, vol. 24, no. 3, pp. 705–716, Mar. 2020, doi: 10.1109/JBHI.2019.2925036.
[18] M. Á. Goda, T. Telek, and F. Kovács, "Novel phonography-based measurement for fetal breathing movement in the third trimester," *Sensors*, vol. 21, no. 1, p. 211, Dec. 2020, doi: 10.3390/s21010211.
[19] A. Haghighi-Mood and J. N. Torry, "A sub-band energy tracking algorithm for heart sound segmentation," *Comput. Cardiol.*, vol. 2, pp. 501–504, Dec. 1995, doi: 10.1109/CIC.1995.482711.
[20] A. Sbrollini, "Fetal phonocardiogram denoising by wavelet transformation: Robustness to noise," in *Proc. Comput. Cardiol.*, vol. 44, 2017, pp. 1–4, doi: 10.22489/CinC.2017.331-075.
[21] M. A. Goda and P. Hajas, "Morphological determination of pathological PCG signals by time and frequency domain analysis," in *Proc. Comput. Cardiol. Conf. (CinC)*, Vancouver, BC, Canada, Sep. 2016, pp. 1133–1136.
[22] D. Kumar, P. Carvalho, M. Antunes, J. Henriques, A. Sa e Melo, and J. Habetha, "Heart murmur recognition and segmentation by complexity signatures," in *Proc. 30th Annu. Int. Conf. IEEE Eng. Med. Biol. Soc.*, Aug. 2008, pp. 2128–2132.
[23] F. Kovacs, C. Horváth, Á. T. Balogh, and G. Hosszá, "Extended noninvasive fetal monitoring by detailed analysis of data measured with phonocardiography," *IEEE Trans. Biomed. Eng.*, vol. 58, no. 1, pp. 64–70, Jan. 2011, doi: 10.1109/TBME.2010.2071871.

MÁRTON ÁRON GODA (Member, IEEE) received the M.Sc. degree in info-bionics engineering from the Faculty of Information Technology and Bionics, Pázmány Péter Catholic University, Budapest, Hungary, in 2015, where he is currently pursuing the Ph.D. degree. His research interest includes biomedical signal processing, especially data-processing methods for large amounts of measurement and analysis of fetal heart sound signals.

TAMÁS TELEK received the degree from the University of Medicine, Novi Sad, Serbia, in 2004, and the Ph.D. degree from Semmelweis University, Budapest, in 2009. In 2018, he specialized as an Endocrinologist. He currently works as the Deputy Head of the Obstetrics and Gynaecology Department with St. Margaret Hospital, Budapest. He is a member of the Hungarian Society Obstetrics Gynaecology, the Hungarian Society for Gynaecological Endoscopy, and the Hungarian Society of Obstetrics and Gynaecology Ultrasound.